Ultrasound Tomography Calibration Using Structured Matrix Completion

Amin Karbasi (1), Sewoong Oh (2), Reza Parhizkar (1) and Martin Vetterli (1,3) *

(1) LCAV, School of Computer and Communication Sciences, EPFL, Switzerland
(2) Department of Electrical Engineering, Stanford University, CA 94305, USA
(3) Department of Electrical Engineering and Computer Sciences, University of California, Berkeley, USA
* Author names appear in alphabetical order

ABSTRACT

Calibration of ultrasound tomography devices is a challenging problem and of highly practical interest in medical and seismic imaging. This work addresses the position calibration problem in circular apertures where sensors are arranged on a circular ring and act both as transmitters and receivers. We introduce a new method of calibration based on the time-of-flight (ToF) measurements between sensors when the enclosed medium is homogeneous. Knowing all the pairwise ToFs, one can find the positions of the sensors using multi-dimensional scaling (MDS) method. In practice, however, we are facing two major sources of loss. One is due to the transitional behaviour of the sensors, which makes the ToF measurements for close-by sensors unavailable. The other is due to the random malfunctioning of the sensors, that leads to random missing ToF measurements. On top of the missing entries, since in practice the impulse response of the piezoelectric and the time origin in the measurement procedure are not present, a time mismatch is also added to the measurements. In this work, we first show that a matrix defined from all the ToF measurements is of rank at most four. In order to estimate the structured and random missing entries, utilizing the fact that the matrix in question is shown to be low-rank, we apply a state-of-the-art low-rank matrix completion algorithm. Then we use MDS in order to find the correct positions of the sensors. To confirm the functionality of our method in practice, simulations mimicking the measurements of an ultrasound tomography device are performed.

INTRODUCTION

Ultrasound tomography aims to evaluate certain features of a medium by using ultrasound waves and characterizing the sound propagation inside the medium. This process can be divided into the following stages; one requires to have

- a reliable setup for obtaining the measurements.
- a proper forward model imitating the setup characteristics.
- an accurate inverse model based on which characterizations of the medium can be estimated.

Often, the forward model might be as well used in the inverse process [1].

The aforementioned forward and inverse models, are mostly based on two different approaches: a) the full wave equation for the forward and inverse problems [2–6], b) ray model for propagation of sound [7, 8]. In both cases, modelling the experimentalf environment is of great importance for the forward and inverse procedures. One of the key elements of these models is the position of the ultrasound sensors in the measurement setup. In order to obtain accurate measurements, the tomography model must be calibrated with the exact sensor locations prior to the experiment.

One way to find the correct sensor positions is to use the time-of-flight (ToF) of ultrasound signals, which is the time taken by an ultrasound wavefront to travel from a transmitter to a receiver. If we have all the ToF measurements between all pairs of sensors when the enclosed medium is homogeneous, then we can construct a ToF matrix where each entry corresponds

to the ToF measurement between each pair of sensors. We can infer the positions of the sensors using this ToF matrix.

Acoustic tomography based on ToF estimation has been used mostly in seismology to determine the sound speed distribution of the earth layers [9]. Recently, investigations are also performed on the usage of ultrasound tomography in temperature and wind estimation [10]. Moreover, recent studies show the benefits of ultrasound tomography in detection and diagnosis of breast cancer [11, 12]. Accordingly, some transmission and reflection ultrasound scanners for measuring the parameters in vivo have been developed. More details can be found in the work of Carson et al. [12], Johnson et al. [13], and Duric et al. [14].

The assumed model in this work is based on the circular tomography devices which are used in [10, 14]. These devices consist of a circular ring surrounding an object and scanning horizontal planes. Ultrasound sensors are placed on the interior boundary of the ring and act as both transmitters and receivers.

To obtain the ToF entries appropriate for our purpose we assume that no object is placed inside the ring. One can think of this stage as the calibration procedure prior to actual experiments.

There are a number of challenges we are encountering in this work, namely,

- the ToF matrices obtained in a practical setup has missing entries.
- the measured entries of the ToF matrices are corrupted

by noise.

- there is an unknown time mismatch added to the measurements.

If one had the complete and noiseless ToF matrix without time mismatch, the task of finding the exact positions would be very simple. This problem has been address in literature as the multi dimensional scaling (MDS) [15]. Unfortunately, the ToF matrix in such setups is never complete and many of the time-of-flight values are missing. The missing entries can be divided into two categories; the first category is the structured missing entries caused by inability of the sensors to compute their mutual time-of-flights with their close by neighbours, and the second category is the random missing entries due to random malfunctioning of the sensors or the ToF estimation software during the measurement procedure.

A good estimation of the positions of the sensors can be obtained, if we have a good estimation of the missing entries of the ToF matrix. In general, it is a difficult task to infer missing entries of a matrix. However, it has recently been discovered that if the matrix has low rank, a small random subset of its entries allow to reconstruct it exactly. This result was first proved by Candes and Recht who analyzed a convex relaxation of this low-rank matrix completion problem [16]. More recently, an alternative approach using a combination of spectral techniques and manifold optimization was introduced in [17]. This novel algorithm used in our work is referred as OPTSPACE and has been shown to be stable under noisy measurements [18]. Since the ToF matrix, when the entries are squared ToF measurements, has low rank, its missing entries can be accurately estimated using OPTSPACE.

On top of the missing entries, we also need to deal with the time mismatch. Since, in practice, the impulse response of the piezoelectric and the time origin in the measurement procedure are not present, an unknown time mismatch is added to the measurements. To infer this time mismatch simultaneously as the positions of the sensors, we propose a recursive algorithm based on OPTSPACE.

We state theoretical bounds on the performance of our proposed method under mild assumptions, however all the proofs are omitted in this paper and interested readers are referred to our technical report. The main focus of this work is on the practicality of our proposed method. For this reason, simulations mimicking the measurements of an ultrasound tomography device are reported.

The organization of this paper is as follows; First, we define the exact model of the problem and the process of dimension reduction is introduced, the process of obtaining the time-of-flights is discussed and the sources of missing entries are described. The next section provides the precise mathematical model of the problem. Then, we explain the OPTSPACE algorithm adapted to this problem. Afterwards, the fundamentals of the position reconstruction from the ToF matrix is discussed and a measure of reconstruction quality is introduced. Later, the main results of this paper in terms of the position reconstruction and the reconstruction error bounds are provided and finally some experimental results are presented.

CIRCULAR TOMOGRAPHY

The focus of this research is ultrasound tomography with circular apertures. In this setup, n ultrasound transmitters and receivers are installed on the interior edge of a circular ring and an object with unknown acoustic characteristics is placed inside the ring. At each time instance a transmitter is fired, sending ultrasound signals with frequencies ranging from hundreds

to thousands of kHz, and all the other sensors on the ring record the signal reaching to their membrane. The same process is repeated for all the transmitters. Each one of n sensors on the ring is capable of transmitting and receiving ultrasound signals. The aim of tomography in general is to use the recorded signals in order to reconstruct the characteristics of the enclosed object (e.g., sound speed, sound attenuation, etc.). The general configuration for such a tomography device is depicted in Fig. 1. Employing these measurements, an inverse problem is constructed, whose solution provides the acoustic characteristics of the enclosed object.
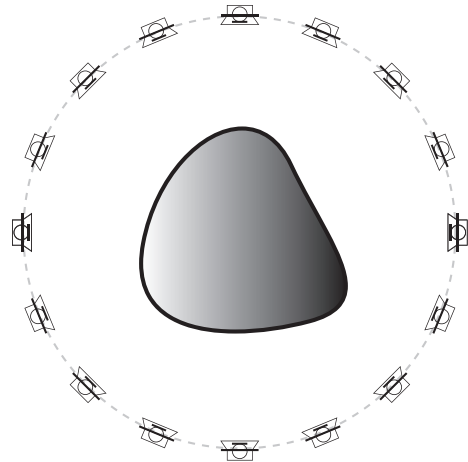

Figure 1: Circular setup for ultrasound tomography considered in this work. Ultrasound transducers are distributed on the edge of a circular ring and the object with unknown characteristics is put inside. Sensors are fired each in turn and the rest of sensors record the ultrasound signals reaching them.

There are two common methods for solving the inverse problem. The solutions are either based on the wave equation [2] or the bent-ray theory [7]. Both techniques consist of forward modelling the system and comparing the simulation results with the measured data. For the detailed explanation of the methods we refer interested readers to [2] and [7]. Nevertheless In both cases, in order to simulate the forward model and rely on the recorded data, very precise measurements of the sensor positions are needed. In most applications (e.g., [1, 19, 20]) it is assumed that the sensors are positioned equidistance apart on a circle and no later calibration is performed to find the exact sensor positions. The main objective of this paper is to estimate the precise positions of the sensors.

Homogeneous Medium

In order to estimate the sensor positions, we use the bent-ray tomography technique. In this method, the region of interest is descretized and an unknown sound speed c_i is associated to each tile in the region. Once each transmitter is fired and receivers recorded the signals, the relative time-of-flights (ToF) between the pairs of transmitters and receivers will be measured. Afterwards, a non-linear set of equations is constructed as below

$$\mathscr{L}(\boldsymbol{x}) = \boldsymbol{T}, \tag{1}$$

where $\mathscr{L}(\boldsymbol{x})$ is a nonlinear transform which relates the lengths of the bent-rays from a transmitter to a receiver to the travel time between them. More precisely, the input of this nonlinear transform is the vector $\boldsymbol{x}$ whose i-th entry x_i, is the inverse of the sound speed in the i-th tile and the output is the ToFs between each pair of sensors.

For estimating the sensor positions, we assume that we have the measurements for ToFs when there is no object inside the

ring. This means that x is constant with values $x_i = 1/c_0$, where c_0 is the sound speed in a homogeneous medium (e.g., water in the context of breast cancer detection) and entries of T represent the time travelled by sound in a straight line between each pair of a transmitter and receiver.

Knowing the the medium temperature and the characteristics of the medium inside the ring, one can accurately estimate the sound speed c_0. Thus, it is reasonable to assume that c_0 is fixed and known. Having the ToFs for a homogeneous medium where no object is placed inside the ring, we can construct a distance matrix D consisting of the mutual distances between the sensors as

$$D = [d_{i,j}] = c_0 T, \qquad T = [t_{i,j}], \quad i,j \in \{1, \cdots, n\} \quad (2)$$

where $t_{i,j}$ is the ToF between sensors i and j and n is the total number of sensors around the circular ring. Notice that the only difference between the ToF matrix T, and distance matrix D, is the constant c_0. This is why in the sequel our focus will mainly be on the distance matrix rather than the actual measured matrix T.

Dimensionality Reduction

Since the enclosed medium is homogeneous, the matrix T is a symmetric matrix with zeros on the diagonal and so is the matrix D. Even though, the distance matrix D is full rank in general, a simple point-wise transform of its entries will lead to a low rank matrix. More precisely, we can prove the following lemma

Lemma 1. If one constructs the squared distance matrix $\bar{D}$ as

$$\bar{D} = D \odot D = \left[d_{i,j}^2\right], \qquad (3)$$

then the matrix $\bar{D}$ has rank at most 4 and if the sensors are placed on a circle, the rank is exactly 3.

In reality, as we will explain in the next section, many of the the entries of the ToF matrix (or equivalently the distance matrix) are missing and there is an unknown time mismatch added to all the measurements.

Time of Flight Estimation

Several methods for ToF estimation have been proposed in the signal processing community [7, 8]. These methods are also known as time-delay estimation in acoustic literature [21, 22]. In all these methods, the received signal is compared to a reference signal (generally the sent signal), and the relative delay is estimated between the two signals. However, this assumption is not true in our case. Normally, each transmitter is fed by an electrical short pulse and this pulse, convolved with the unknown transfer function of the transducer, constructs the sent signal. Unless we have measurements exactly on the transducer membrane, we are not able to find the exact shape of the sent signal. Thus, there is not any reference signal to find the relative time-of-flights.

Because of above limitations, we are forced to estimate the *absolute* ToFs. For this purpose, we will use first arrival method. This method probes the received signal and defines the time-of-flight as the time instant at which the received signal power exceeds a predefined threshold.

In the practical screening systems, to record measurements for one fired transmitter, all the sensors are turned on simultaneously and after some unknown transition time (which is caused by the system structure, different sensor responses, etc.), the transmitter is fed with the electrical signal and the receivers

start recording the signal. This unknown time may change for each pair of transmitters and receivers. We will see that this unknown time shift plays an important role in sensor position estimation.

The transition behaviour prevents the transducers from responding to the received signal immediately after being turned on. This results in the lack of correct ToF measurements for the sensors positioned close to each other. Therefore, numbering the sensors on the ring from 1 to n, in the ToF matrix T, we will not have measurements on a certain band around the main diagonal and on the lower left and upper right parts as well. We call these missing entries as *structured missing entries*.

During the measurement procedure, it may also happen that some sensors do not act correctly and give outliers. Thus, as in [23], a post processing is also performed on the measurements, in which a smoothness criteria is defined and the measurements which do not satisfy this criteria are removed from the ToF matrix. We address these entries as *random missing entries*. The following figure illustrates one instance of the ToF matrix with these random effects, where T_{inc} denotes the incomplete ToF matrix and the grey entries correspond to the missing entries.
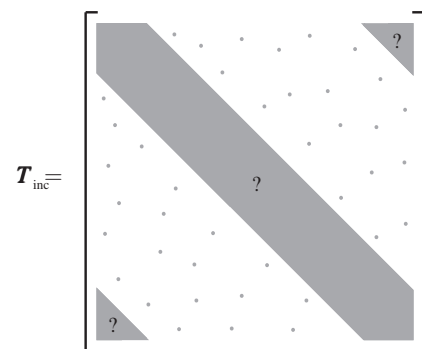
Furthermore, in practice, the measurements are corrupted by noise.

The above mentioned problems result in an incomplete matrix T, which cannot be used for position reconstruction, unless the mismatch effect is removed and the unknown entries are estimated.

PROBLEM SETTING

We observed that the distance matrix when there is only water inside the screening aperture can be calculated as in (2). We also saw in the previous section that the measurements for ToF matrix T have three major problems : they are noisy, some of them are missing, and the measurements are added with some unknown time delay. For simplicity, we will assume that this time delay is constant for all the transmitters, namely all the transmitters send the electrical signal after some fixed but unknown delay t_0. Hence, we can rewrite the ToF matrix as follows

$$\tilde{T} = T + t_0 A + Z_0, \qquad (4)$$

where T consists of ideal measurements for ToF, Z_0 is the noise matrix and A is defined as

$$A = [a_{i,j}], \quad a_{i,j} = \begin{cases} 1 & \text{if } i \neq j \\ 0 & \text{otherwise} \end{cases} \qquad (5)$$

With the above considerations, the distance matrix can also be written as

$$\tilde{D} = D + d_0 A + Z, \qquad (6)$$

where $D = c_0 T$, $d_0 = c_0 t_0$, and $Z = c_0 Z_0$.

In our model we no longer assume that the sensors are placed exactly on the ring. What happens in practice is that the sensor positions deviate from the circumference and our ultimate goal is to estimate these deviations or equivalently the correct positions (see Fig. 2). The general positions taken by sensors are denoted by the set of vectors $\{\boldsymbol{x}_1, \ldots, \boldsymbol{x}_n\}$.
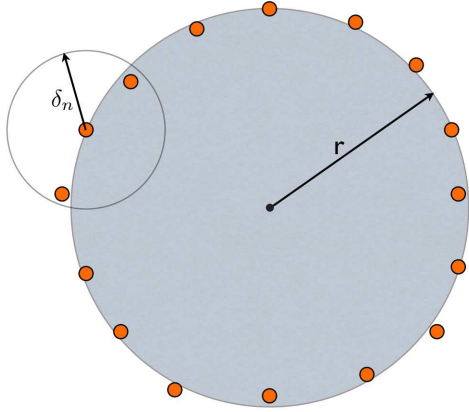

Figure 2: Sensors are distributed around a circle of radius r with small deviations from the circumference.

As described earlier, there are two contributions of missing entries. One is the missing measurements of close-by sensors, which we call *structured missing entries*. The other is the missing measurements due to random malfunction of sensors, which we call *random missing entries*. First to incorporate the structured missing entries, we assume that any measurements between sensors of distance less than δ_n are missing (see Figure 2). The number of structured missing entries depends on the choice of δ_n. In the real tomography data, we only have a few structured missing entries per row. We are interested in the regime where we have a small number of structured missing entries per row in the large systems limit. Accordingly, typical range of δ_n of interest is $\delta_n = \Theta(r \log n/n)$. A random set of structured missing indices $S \subseteq [n] \times [n]$ is defined from $\{\boldsymbol{x}_i\}$ and δ_n, by

$$S = \{(i,j): \ d_{i,j} \leq \delta_n \text{ and } i \neq j\}, \tag{7}$$

where $d_{i,j} = ||\boldsymbol{x}_i - \boldsymbol{x}_j||$. Then, the structured missing entries are denoted by a matrix

$$\boldsymbol{D}^s_{i,j} = \begin{cases} \boldsymbol{D}_{i,j} & \text{if } (i,j) \in S, \\ 0 & \text{otherwise}. \end{cases} \tag{8}$$

Note that the matrix $\boldsymbol{D}^{\bar{s}} = \boldsymbol{D} - \boldsymbol{D}^s$ captures the noiseless distance measurements that is not effected by structured missing entries. This way, we can interpret the matrix $\boldsymbol{D}^s$ as additive noise in our model. Likewise, for the time mismatch we can define

$$\boldsymbol{A}^{\bar{s}}_{i,j} = \begin{cases} \boldsymbol{A}_{i,j} & \text{if } (i,j) \in S^\perp, \\ 0 & \text{otherwise}, \end{cases} \tag{9}$$

where $S^\perp$ denotes the complementary set of S. Next, to model the noise we add a random noise matrix $\boldsymbol{Z}^{\bar{s}}$.

$$\boldsymbol{Z}^{\bar{s}}_{i,j} = \begin{cases} \boldsymbol{Z}_{i,j} & \text{if } (i,j) \in S^\perp, \\ 0 & \text{otherwise}. \end{cases} \tag{10}$$

We do not assume a prior distribution on $\boldsymbol{Z}$, and the main theorem is stated for any general noise matrix $\boldsymbol{Z}$, deterministic or random. One practical example of $\boldsymbol{Z}$ is an i.i.d. Gaussian model.

Finally, to model the random missing entries, we assume that each entry of $\boldsymbol{D}^{\bar{s}} + t_0 c_0 \boldsymbol{A}^{\bar{s}} + \boldsymbol{Z}^{\bar{s}}$ is sampled with probability p_n. In the calibration data, we typically see a small number of random missing entries. Hence, in order to model it we assume that $p_n = \theta(1)$. Let $E \subseteq [n] \times [n]$ denote the subset of indices which are not erased by random missing entries. Then a projection $\mathscr{P}_E : \mathbb{R}^{n \times n} \rightarrow \mathbb{R}^{n \times n}$ is defined as

$$\mathscr{P}_E(\boldsymbol{M})_{i,j} = \begin{cases} \boldsymbol{M}_{i,j} & \text{if } (i,j) \in E, \\ 0 & \text{otherwise}. \end{cases} \tag{11}$$

We denote the observed measurement matrix by

$$\boldsymbol{N}^E = \mathscr{P}_E(\boldsymbol{D}^{\bar{s}} + d_0 \boldsymbol{A}^{\bar{s}} + \boldsymbol{Z}^{\bar{s}}), \tag{12}$$

where $d_0 = t_0 c_0$ is a constant. Notice that the matrix $\boldsymbol{N}^E$ has the same shape as $\boldsymbol{T}_{\text{inc}}$ shown already schematically.

Goal: Given this observed matrix $\boldsymbol{N}^E$ and the missing indices $S \cup E^\perp$, we want to estimate a matrix $\hat{\boldsymbol{D}}$ which is very close to the correct distance matrix $\boldsymbol{D}$. Then by using $\hat{\boldsymbol{D}}$ we would like to be able to estimate the sensor positions.

In order to achieve this goal, there are two obstacles we need to overcome. First, how to estimate the missing entries of $\boldsymbol{N}^E$ and second, how to find the sensor positions given approximate pairwise distances. The former is done by deploying the matrix completion algorithm and the latter by using the multidimensional scaling.

MATRIX COMPLETION

OPTSPACE, introduced in [17], is an algorithm for recovering a low-rank matrix from noisy data with missing entries. The steps are shown in Algorithm 1. Let $\boldsymbol{M}$ be a rank-q matrix of dimensions $n \times n$, $\boldsymbol{Z}$ the measurement noise, and E the set of indices of the measured entries. Then, the measured noisy and incomplete matrix is $\boldsymbol{M}^E = \mathscr{P}_E(\boldsymbol{M} + \boldsymbol{Z})$.

Algorithm 1 OPTSPACE

Input: Observed matrix $\boldsymbol{M}^E = \mathscr{P}_E(\boldsymbol{M} + \boldsymbol{Z})$.
Output: Estimate $\boldsymbol{M}$.
  1: Trimming: remove over-represented columns/rows;
  2: Rank-q projection on the space of rank-q matrices according to (13);
  3: Gradient descent: Minimize a cost function $F(\cdot)$ defined in [17];

In the trimming step, a row or a column is over-represented if it contains more samples than twice the average number of samples per row or column. These rows or columns can dominate the spectral characteristics of the observed matrix $\boldsymbol{M}^E$, and are removed from the observed matrix. Let $\tilde{\boldsymbol{M}}^E$ be the resulting matrix of this trimming step. This trimming step is presented here for completeness, but in the case when p_n is larger than some fixed constant (like in our case where $p_n = \Theta(p)$), $\boldsymbol{M}^E = \tilde{\boldsymbol{M}}^E$ with high probability and the trimming step can be omitted.

In the second step, we first compute the singular value decomposition (SVD) of $\tilde{\boldsymbol{M}}^E$.

$$\tilde{\boldsymbol{M}}^E = \sum_{i=1}^n \sigma_i(\tilde{\boldsymbol{N}}^E) u_i v_i^T,$$

where $\sigma_i(\cdot)$ denotes the i-th singular value of a matrix. Then, the rank-q projection returns the matrix

$$\mathscr{P}_q(\tilde{\boldsymbol{M}}^E) = (1/p_n) \sum_{i=1}^q \sigma_i(\tilde{\boldsymbol{M}}^E) u_i v_i^T, \tag{13}$$

obtained by setting to 0 all but the q largest singular values.

Starting from the initial guess provided by the rank-q projection $\mathscr{P}_q(\tilde{\boldsymbol{M}}^E)$, the final step minimizes the cost function $F(\cdot)$ defined in [17] using a gradient descent method. This last step tries to get us as close as possible to the correct low rank matrix $\boldsymbol{M}$.

POSITION RECONSTRUCTION

Even if we had a good estimate of $\boldsymbol{D}$, how we would position the sensors is not a trivial question. Multidimensional scaling (MDS) is a technique used in finding the configuration of objects in a low dimensional space such that the measured pairwise distances are preserved. If all the pairwise distances are measured without error then a naive application of MDS exactly recovers the configuration of sensors [15, 24, 25].

Algorithm 2 Classical Metric MDS [25].

Input: Dimension d, estimated squared distance matrix $\bar{\boldsymbol{D}}$
Output: Estimated positions $\mathsf{MDS}_d(\bar{\boldsymbol{D}})$
 1: Compute $(-1/2)\boldsymbol{L}\bar{\boldsymbol{D}}\boldsymbol{L}$, where $\boldsymbol{L} = \mathbb{I}_n - (1/n)\mathbb{1}_n\mathbb{1}_n^T$;
 2: Compute the best rank-d approximation $\boldsymbol{U}_d\boldsymbol{\Sigma}_d\boldsymbol{U}_d^T$ of $(-1/2)\boldsymbol{L}\bar{\boldsymbol{D}}\boldsymbol{L}$;
 3: Return $\mathsf{MDS}_d(\bar{\boldsymbol{D}}) \equiv \boldsymbol{U}_d\boldsymbol{\Sigma}_d^{1/2}$.

There are various types of MDS techniques, but, throughout this paper, by MDS we refer to the classical metric MDS, which is defined as follows. Let L be an $n \times n$ symmetric matrix such that

$$\boldsymbol{L} = \mathbb{I}_n - (1/n)\mathbb{1}_n\mathbb{1}_n^T, \tag{14}$$

where $\mathbb{1}_n \in \mathbb{R}^n$ is the all ones vector and $\mathbb{I}_n$ is the $n \times n$ identity matrix. Let $\mathsf{MDS}_d(\bar{\boldsymbol{D}})$ denote the $n \times d$ matrix returned by MDS when applied to the squared distance matrix $\bar{\boldsymbol{D}}$. The task is to embed n objects in a d dimensional space $\mathbb{R}^d$. In our case for instance, where we want to find the position of sensors on a two dimensional space, we have $d = 2$. Then, in formula, given the singular value decomposition (SVD) of a symmetric and positive semidefinite matrix $(-1/2)\boldsymbol{L}\bar{\boldsymbol{D}}\boldsymbol{L}$ as $(-1/2)\boldsymbol{L}\bar{\boldsymbol{D}}\boldsymbol{L} = \boldsymbol{U}\boldsymbol{\Sigma}\boldsymbol{U}^T$,

$$\mathsf{MDS}_d(\bar{\boldsymbol{D}}) \equiv \boldsymbol{U}_d\boldsymbol{\Sigma}_d^{1/2},$$

where $\boldsymbol{U}_d$ denotes the $n \times d$ left singular matrix corresponding to the d largest singular values and $\boldsymbol{\Sigma}_d$ denotes the $d \times d$ diagonal matrix with d largest singular values in the diagonal. This is also known as the MDSLOCALIZE algorithm in [15]. Note that since the columns of $\boldsymbol{U}$ are orthogonal to $\mathbb{1}_n$ by construction, it follow that $\boldsymbol{L} \cdot \mathsf{MDS}_d(\bar{\boldsymbol{D}}) = \mathsf{MDS}_d(\bar{\boldsymbol{D}})$.

It can be easily shown that when MDS is applied to the correct and complete squared distance matrix without noise, the configuration of sensors are exactly recovered [15]. This follows from the following equality

$$-\frac{1}{2}\boldsymbol{L}\bar{\boldsymbol{D}}\boldsymbol{L} = \boldsymbol{L}\boldsymbol{X}\boldsymbol{X}^T\boldsymbol{L}, \tag{15}$$

where $\boldsymbol{X}$ denotes the $n \times d$ position matrix in which the i-th row corresponds to $\boldsymbol{x}_i$, the d dimensional position vector of sensor i. Note that we only get the configuration and not the absolute positions, in the sense that $\mathsf{MDS}_d(\bar{\boldsymbol{D}})$ is one version of infinitely many solutions that matches the distance measurements $\boldsymbol{D}$. Intuitively, it is clear that the pairwise distances are invariant to a rigid transformation (a combination of rotation, reflection and translation) of the positions $\boldsymbol{X}$, and therefore there are multiple instances of $\boldsymbol{X}$ that result in the same $\boldsymbol{D}$. For future use, we introduce a formal definition of rigid transformation and related terms.

Denote by $\mathsf{O}(d)$ the group of orthogonal $d \times d$ matrices. A set of sensor positions $\boldsymbol{Y} \in \mathbb{R}^{n \times d}$ is a rigid transform of $\boldsymbol{X}$, if there exists a d-dimensional shift vector s and an orthogonal matrix $\boldsymbol{Q} \in \mathsf{O}(d)$ such that

$$\boldsymbol{Y} = \boldsymbol{X}\boldsymbol{Q} + \mathbb{1}_n s^T .$$

$\boldsymbol{Y}$ should be interpreted as a result of first rotating (and/or reflecting) sensors in position $\boldsymbol{X}$ by $\boldsymbol{Q}$ and then adding a shift by s. Similarly, when we say two position matrices $\boldsymbol{X}$ and $\boldsymbol{Y}$ are equal up to a rigid transformation, we mean that there exists a rotation $\boldsymbol{Q}$ and a shift s such that $\boldsymbol{Y} = \boldsymbol{X}\boldsymbol{Q} + \mathbb{1}_n s^T$. Also, we say a function $f(\boldsymbol{X})$ is invariant under rigid transformation if and only if for all $\boldsymbol{X}$ and $\boldsymbol{Y}$ that are equal up to a rigid transformation, we have $f(\boldsymbol{X}) = f(\boldsymbol{Y})$. Under these definitions, it is clear that $\boldsymbol{D}$ is invariant under rigid transformation, since for all (i,j), $\boldsymbol{D}_{ij} = ||\boldsymbol{x}_i - \boldsymbol{x}_j|| = ||(\boldsymbol{x}_i\boldsymbol{Q} + s^T) - (\boldsymbol{x}_j\boldsymbol{Q} + s^T)||$, for any $\boldsymbol{Q} \in \mathsf{O}(d)$ and $s \in \mathbb{R}^d$.

Let $\hat{\boldsymbol{X}}$ denote an $n \times d$ estimation for $\boldsymbol{X}$ with estimated position for sensor i in the i-th row. Then, we need to define a metric for the distance between the original position matrix $\boldsymbol{X}$ and the estimation $\hat{\boldsymbol{X}}$ which is invariant under rigid transformation of $\boldsymbol{X}$ or $\hat{\boldsymbol{X}}$.

The matrix $\boldsymbol{L}$ defined in (14) is a symmetric matrix with rank $n-1$ which eliminates the contributions of the translation. More precisely,

$$\boldsymbol{L}\boldsymbol{X} = \boldsymbol{L}(\boldsymbol{X} + \mathbb{1}s^T),$$

for all $s \in R^d$. We can show that $\boldsymbol{L}$ has the following properties.

Lemma 2. [15, 25, 26] Let the matrix $\boldsymbol{L}$ be defined as in (14). Moreover, let $\boldsymbol{X}$ and $\hat{\boldsymbol{X}}$ be two position matrices with dimension $n \times d$. Then, we can show that

- $\boldsymbol{L}\boldsymbol{X}\boldsymbol{X}^T\boldsymbol{L}$ is invariant under rigid transformation.
- $\boldsymbol{L}\boldsymbol{X}\boldsymbol{X}^T\boldsymbol{L} = \boldsymbol{L}\hat{\boldsymbol{X}}\hat{\boldsymbol{X}}^T\boldsymbol{L}$ implies that $\boldsymbol{X}$ and $\hat{\boldsymbol{X}}$ are equal up to a rigid transformation.

This naturally defines the following distance between $\boldsymbol{X}$ and $\hat{\boldsymbol{X}}$.

$$d_1(\boldsymbol{X}, \hat{\boldsymbol{X}}) = \frac{1}{n}\left|\left|\boldsymbol{L}\boldsymbol{X}\boldsymbol{X}^T\boldsymbol{L} - \boldsymbol{L}\hat{\boldsymbol{X}}\hat{\boldsymbol{X}}^T\boldsymbol{L}\right|\right|_F, \tag{16}$$

where $||\cdot||_F$ denotes the Frobenius norm.

According to Lemma 2 this distance is invariant to rigid transformation of $\boldsymbol{X}$ and $\hat{\boldsymbol{X}}$. Furthermore, $d_1(\boldsymbol{X}, \hat{\boldsymbol{X}}) = 0$ implies that $\boldsymbol{X}$ and $\hat{\boldsymbol{X}}$ are equal up to a rigid transformation. We later state our theoretical results in terms of the distance defined in (16).

MAIN RESULTS

The main reason we cannot apply OPTSPACE on $\boldsymbol{N}^E$ in (12) is the mismatch time. Since $\boldsymbol{A}$ is a full rank matrix, the matrix $\tilde{\boldsymbol{D}} \odot \tilde{\boldsymbol{D}}$ no longer has rank four. Therefore, our main concern is to estimate the value d_0 and subtract it from the observed entries of $\boldsymbol{N}^E$. Since the measurements are noisy, one cannot hope for estimating the exact value of d_0. Hence, we propose an iterative algorithm for estimating the value of d_0.

In fact, the above algorithm guarantees that after removing the effect of the time-mismatch, we have found best rank 4 approximation of the distance squared matrix. In other words, if we remove exactly the mismatch d_0, we will have an incomplete version of a rank 4 matrix and after reconstruction, the measured values will be close to the reconstructed ones.

For the following theorems, we assume that our estimation for d_0 is good and we can subtract the mismatch term in $\boldsymbol{N}^E$. Therefore, the resulting matrix can be approximated by using the matrix completion algorithm OPTSPACE.

Algorithm 3 Finding d_0.

Input: Matrix $\mathbf{N}^E$;
Output: Estimate d_0;

1: Construct the candidate set $\mathscr{C}_d = \{d_0^{(1)}, \ldots, d_0^{(M)}\}$ containing discrete values for d_0.
2: **for** $k = 1$ to M **do**
3:      Set $\mathbf{N}_{(k)}^E = \mathbf{N}^E - d_0^{(k)} A^E$;
4:      Set $\bar{\mathbf{N}}_{(k)}^E = \mathbf{N}_{(k)}^E \odot \mathbf{N}_{(k)}^E$;
5:      Apply OPTSPACE on $\bar{\mathbf{N}}_{(k)}^E$ and call the output $\hat{\mathbf{N}}^{(k)}$;
6:      Apply MDS and let $X^{(k)} = MDS_2(\hat{\mathbf{N}}^{(k)})$;
7:      Find $c^{(k)}$
$$c^{(k)} = \sum_{(i,j) \in E \cap S^\perp} \left(d_0^{(k)} + \|X_i^{(k)} - X_j^{(k)}\| - \mathbf{N}_{i,j}^E \right)^2;$$
8: **end for**
9: Find d_0 satisfying
$$d_0 = d_0^{(l)}, \quad l = \arg\min_k c^{(k)};$$

Theorem 1. Assume n sensors are distributed uniformly at random around a circle with radius r. The resulting distance measurement matrix $\bar{\mathbf{D}}$ is corrupted by systematic missing entries $\bar{\mathbf{D}}^s$ and measurement noise $\mathbf{Z}^{\bar{s}}$. Further, the entries are randomly missing with probability p_n. Let $\mathbf{N}^E = \mathscr{P}_E(\bar{\mathbf{D}} - \bar{\mathbf{D}}^s + \mathbf{Z}^{\bar{s}})$ denote the observed matrix. Assume $\delta_n = \delta\, r \log n / n$ and $p_n = p$, where $\delta \in [1, \infty)$ and $p \in [0, 1]$ are constants which do not depend on n. Let $\mathbf{Y}$ be defined from the noise matrix such that $\mathbf{Y}_{i,j} = \mathbf{Z}_{i,j}^2 + 2\mathbf{Z}_{i,j}\mathbf{D}_{i,j}$. Then, there exists constants C_1, C_2, and C_3 such that the output of OPTSPACE $\hat{\mathbf{D}}$ achieves

$$\frac{1}{n}\|\bar{\mathbf{D}} - \hat{\mathbf{D}}\|_F \le C_1 r^2 \left(\frac{\delta \log n}{n}\right)^3 + C_2 \frac{\|\mathscr{P}_E(\mathbf{Y}^{\bar{s}})\|_2}{pn}, \quad (17)$$

with probability larger than $1 - 1/n^3$ provided that the right hand side is less than $C_3 r^2$.

The above theorem, in great generality, holds for any noise matrix Z, deterministic or random. The above guarantees only hold 'up to numerical constants'. To see how good OPTSPACE is in practice, we need to run numerical experiments. For more results supporting the robustness of OPTSPACE, we refer to [27].

Theorem 2. Applying multidimensional scaling algorithm on $\hat{\mathbf{D}}$, the error on the resulting coordinates will be bounded as follows

$$d_1(\hat{\mathbf{X}}, \mathbf{X}) \le C_1 r^2 \left(\frac{\delta \log n}{n}\right)^3 + C_2 \frac{\|\mathscr{P}_E(\mathbf{Y}^{\bar{s}})\|_2}{pn}, \quad (18)$$

with probability larger than $1 - 1/n^3$.

The proofs of all the lemmas and theorems can be found in our technical report.

EXPERIMENTAL RESULTS

In order to evaluate the theoretical results, we have also provided practical evidence. We construct a set of simulations imitating the problem setup. In the sequel, a sensing ring with 200 transducers is assumed to acquire the ultrasound signals. The ring diameter is assumed 10 cm. The setup is close to the one used in [14]. At each time instance a transmitter sends ultrasound signal to the enclosed field and all the other sensors record the measurements.

In the calibration problem, we are interested in the measurements taken with homogeneous medium (for example water as

in [14] or homogeneous air as in [10]). A first set of simulations is done under the fact that there is no noise in the ToF measurements. In this case, the ToF matrix will correspond to the mutual distances between the sensors up to a scale by c_0, the sound speed in the medium. In the simulations, the sound speed is assumed to equal to 1500 m/s. From the ToF matrix, the distance matrix $\tilde{\mathbf{D}}$ is constructed. Afterwards, ε of the entries are removed from the matrix (these correspond to the random missing entries) with positions taken uniformly in the matrix. Then, the measurements smaller than δ are set to zero in $\tilde{\mathbf{D}}$ matrix (these correspond to the structured missing entries). The value for t_0 is also set and all the measurements in the matrix are added by $c_0 t_0$. Afterwards, the elements of the matrix are raised to the power 2 and the new matrix is called $\bar{\mathbf{D}}$. The resulting $\bar{\mathbf{D}}$ matrix is demonstrated in Fig. 3(a). As it is shown in the resulting ToF matrix, we do not have measurements for the ToF between close sensors, this is represented by black bands in the diagonal and the corners of the matrix. Due to the random malfunction of the sensors, some measurements in other regions of the matrix are also removed in the post-processing phase of data acquisition.

In order to complete this matrix and find the time mismatch at the same time, we use the algorithm presented in Algorithm 3. We force the rank of $\bar{\mathbf{D}}$ to 4. The value for t_0 is found as $4\mu s$ which is exactly as set in the simulation. The output of OPTSPACE algorithm is the completed $\bar{\mathbf{D}}$ matrix which is shown in Fig. 3(b).
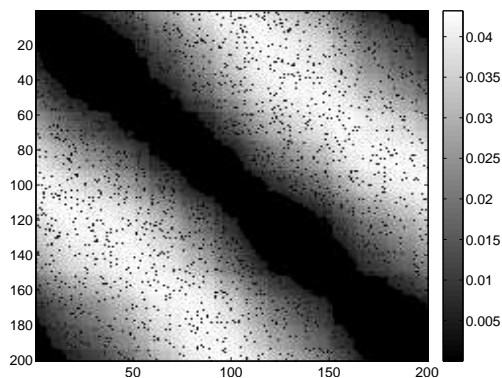
(a) Incomplete distance squared Matrix
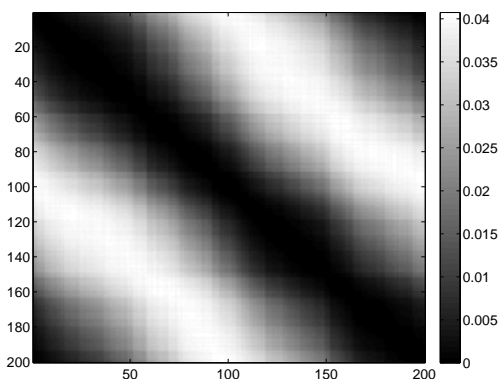
(b) Completed distance squared Matrix

Figure 3: Input and output of OPTSPACE algorithm. Figure (a) shows the incomplete distance squared matrix $\bar{\mathbf{D}}$, with $\varepsilon = 0.05$, $t_0 = 4\mu s$ and $\delta = 7cm$. Figure (b) shows the completed matrix with estimated $t_0 = 4\mu s$. The modified OPTSPACE algorithm in this case can find the time mismatch correctly.

Using the completed distance squared matrix, the MDS algorithm 2 is used to estimate the sensor positions. As discussed in aforementioned section, the positions are estimated up to a

certain translation, reflection and rotation, but the key property which is their order of appearance is preserved in this process. Thus, to be consistent in the figures and comparisons, the estimated positions are translated and rotated so that sensor number one has the same angle as for the uncalibrated corresponding sensor. Note that in the tomography setup the positions and the orientation of the ring does not affect the inverse imaging procedure and all the positions are relative. Then, the distance of the sensors from the center of the circle is calculated and plotted in Fig. 4. From the figure it is obvious that in contrary to the uncalibrated positions, in fact, sensors are off the circle.
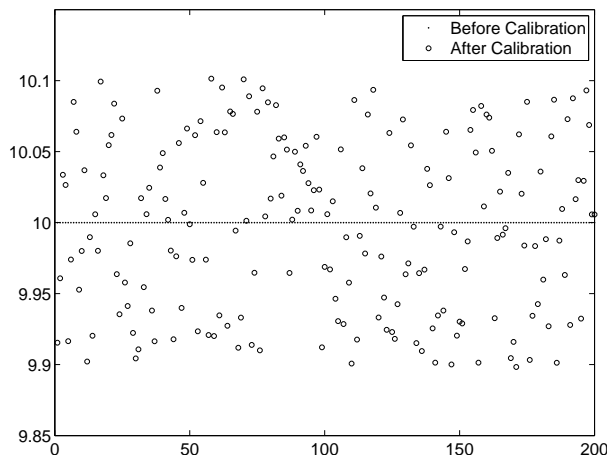

Figure 4: Distance of each sensor from the center of the circle before calibration and after calibration. In practice it is assumed that the sensors are placed on the circle and thus the distance from circle for all of them would be assumed equal to 10 cm in this case, whereas, in reality, they deviate from the circle.

In order to check how much the calibration problem affects the final inversion procedure, another test is performed. Thus, in the next phase of the experiments, the estimated positions are fed to the inverse imaging algorithm. This test basically determines how accurate are the estimated coordinates. Essentially, if the positions were accurate, after the reconstruction of the inside object-which is water in this case- the ring should not appear in the reconstructed image. However, if the positions are not correct, the time-of-flights do not correspond exactly to the positions and this causes a ring to appear in the reconstruction. This effect is shown in Fig. 5(a). In the figure, the results for four reconstructions are presented. In 5(a), the ToF matrix is not complete, it contains the time mismatch t_0, and the positions are not calibrated. The dark gray ring is caused by the non-zero time mismatch in the ToF measurements. In 5(b), the time mismatch is resolved using the proposed algorithm, but the sensor positions are not calibrated and the ToF matrix is still not complete. This figure shows clearly that finding the unknown time mismatch improves significantly the reconstruction image. Figure 5(c), shows the reconstructed image when the ToF matrix is completed and time mismatch is removed, but the sensor positions are not yet calibrated. From this figure, it is confirmed that accurtae time-of-flights are necessary but not sufficient to have a good reconstruction of the inclosed object. Finally, Fig. 5(d) shows the reconstruction when the positions are also calibrated. Comparing the dynamic range of the reconstructed objects, shows how good is the inversion result for the last case.

REFERENCES

[1] F. Natterer, "Acoustic mammography in the time domain," University of Münster, Germany, Tech. Rep., 2008.

[2] F. Natterer and F. Wübbeling, *Mathematical Methods in Image Reconstruction*. SIAM, 2001.

[3] A. C. Kak and M. Slaney, *Principles of Computerized Tomographic Imaging*. Philadelphia, PA, USA: Society for Industrial and Applied Mathematics, 2001.

[4] A. Devaney, "A fast filtered backpropagation algorithm for ultrasound tomography," *Ultrasonics, Ferroelectrics and Frequency Control, IEEE Transactions on*, vol. 34, no. 3, pp. 330–340, 1987.

[5] M. Bronstein, A. Bronstein, M. Zibulevsky, and H. Azhari, "Reconstruction in diffraction ultrasound tomography using nonuniform fft," *Medical Imaging, IEEE Transactions on*, vol. 21, no. 11, pp. 1395–1401, 2002.

[6] S. Johnson, T. Abbott, R. Bell, M. Berggren, D. Borup, D. Robinson, J. Wiskin, S. Olsen, and B. Hanover, "Noninvasive breast tissue characterization using ultrasound speed and attenuation: In vivo validation," in *Acoustical Imaging*. Springer Netherlands, 2007, pp. 147–154.

[7] I. Jovanović, "Inverse problems in acoustic tomography," Ph.D. dissertation, EPFL, Lausanne, 2008.

[8] C. Li, L. Huang, N. Duric, H. Zhang, and C. Rowe, "An improved automatic time-of-flight picker for medical ultrasound tomography," *Ultrasonics*, vol. 49, no. 1, pp. 61 – 72, 2009.

[9] R. R. Stewart, "Exploration seismic tomography: Fundamentals," *Society of Exploration Geophysicists*, 1991.

[10] I. Jovanovic, L. Sbaiz, and M. Vetterli, "Acoustic tomography for scalar and vector fields: theory and application to temperature and wind estimation," *Journal of Atmospheric and Oceanic Technology*, vol. 26, no. 8, pp. 1475 – 1492, 2009.

[11] J. Greenleaf, S. Johnson, and R. Bahn, "Quantitative cross-sectional imaging of ultrasound parameters," in *Ultrasonics Symposium*, 1977, pp. 989–995.

[12] P. Carson, C. Meyer, A. Scherzinger, and T. Oughton, "Breast imaging in coronal planes with simultaneous pulse echo and transmission ultrasound," *Science*, vol. 214, no. 4525, pp. 1141–1143, 1981.

[13] S. A. Johnson, J. W. Wiskin, D. T. Borup, D. A. Christensen, and F. Stenger, "Apparatus and method for imaging with wavefields using inverse scattering techniques," United States Patent No. 5588032, 1996.

[14] N. Duric, P. Littrup, L. Poulo, A. Babkin, R. Pevzner, E. Holsapple, O. Rama, and C. Glide, "Detection of breast cancer with ultrasound tomography: First results with the computed ultrasound risk evaluation (cure) prototype," *Medical Physics*, vol. 34, no. 2, pp. 773–785, 2007.

[15] P. Drineas, A. Javed, M. Magdon-Ismail, G. Pandurangant, R. Virrankoski, and A. Savvides, "Distance matrix reconstruction from incomplete distance information for sensor network localization," in *Sensor and Ad Hoc Communications and Networks*, vol. 2, Sept. 2006, pp. 536–544.

[16] E. J. Candès and B. Recht, "Exact matrix completion via convex optimization," *CoRR*, vol. abs/0805.4471, 2008.

[17] R. H. Keshavan, A. Montanari, and S. Oh, "Matrix completion from a few entries," *IEEE Trans. Inform. Theory*, 2010, arXiv:0901.3150.

[18] ——, "Matrix completion from noisy entries," in *Advances in Neural Information Processing Systems*, December 2009.

[19] I. Jovanović, A. Hormati, L. Sbaiz, and M. Vetterli, "Efficient and Stable acoustic tomography using sparse re-

construction methods," in *19th International Congress on Acoustics*, 2007.

[20] F. Simonetti, L. Huang, and N. Duric, "On the spatial sampling of wave fields with circular ring apertures," *Journal of Applied Physics*, vol. 101, no. 8, p. 083103, 2007.

[21] J. Chen, Y. Huang, and J. Benesty, "Time delay estimation," in *Audio Signal Processing for Next-Generation Multimedia Communication Systems*, Y. Huang and J. Benesty, Eds. Springer US, 2004, ch. 8, pp. 197–227.

[22] R. Parhizkar, "Spatial error concealment in ad-hoc audio conferencing systems," Master's thesis, EPFL, Lausanne, 2009.

[23] I. Jovanović, A. Hormati, O. Roy, and M. Vetterli, "Bent-ray ultrasound tomography with application to breast imaging," to be submitted to IEEE Transactions on Medical Imaging.

[24] J. B. Kruskal and M. Wish, *Multidimensional scaling*. Beverly Hills : SAGE Publications, 1978.

[25] Y. Shang, W. Ruml, Y. Zhang, and M. P. J. Fromherz, "Localization from mere connectivity," in *MobiHoc '03: Proceedings of the 4th ACM international symposium on Mobile ad hoc networking & computing*. New York, NY, USA: ACM, 2003, pp. 201–212.

[26] A. Karbasi and S. Oh, "Distributed sensor network localization from local connectivity : performance analysis for the Hop-Terrain algorithm," in *SIGMETRICS'10: Proceedings of the 2010 ACM SIGMETRICS International Conference on Measurement and Modeling of Computer Systems*, June 2010.

[27] R. H. Keshavan and S. Oh, "Optspace: A gradient descent algorithm on the grassman manifold for matrix completion," 2009, `arXiv:0910.5260`.
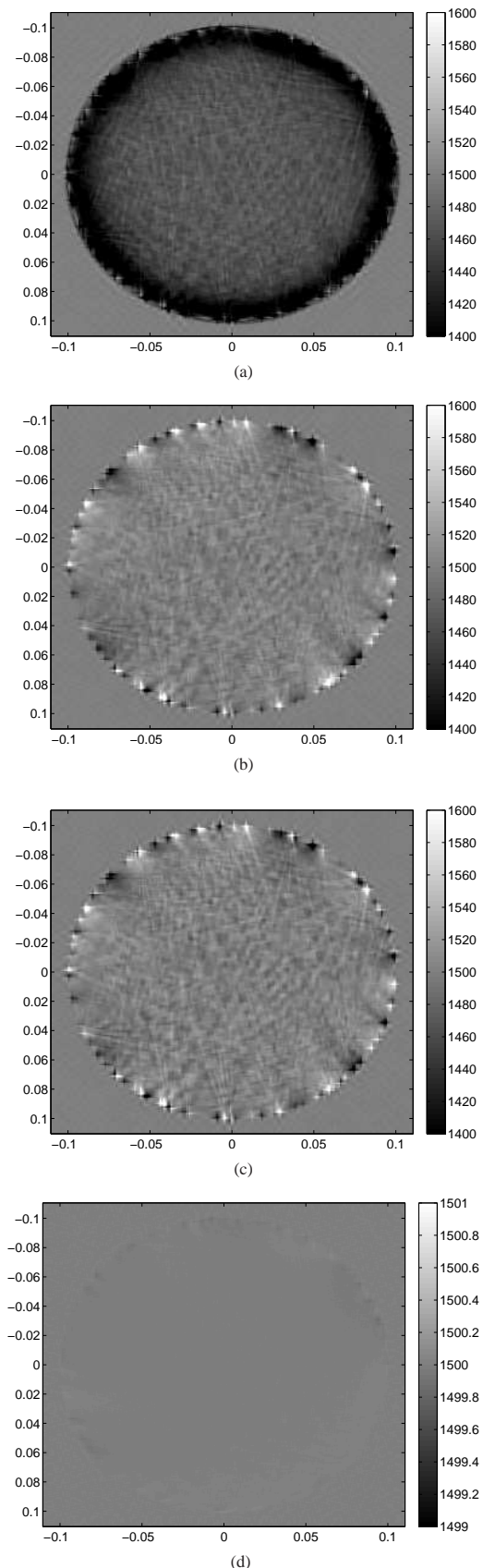

(a)

(b)

(c)

(d)

Figure 5: Results of the inversion procedure for finding the sound speed inside the ring with only water inside. Figure (a) shows the case when no calibration in performed. Fig.(b) is for the case where t_0 is removed from the ToF matrix, but the matrix is still incomplete and the positions are not calibrated. Fig. (c) shows the reconstruction when the matrix is also completed, but the positions are not yet calibrated. Finally, Fig.(d) illustrates the reconstruction with completed ToF matrix and calibrated positions. Note the difference in the dynamic range of the last figure with the others.